AIAA 81-4103

Transonic Viscous-Inviscid Interaction over Airfoils for Separated Laminar or Turbulent Flows

Rachel Gordon* and Josef Rom†
Technion—Israel Institute of Technology, Haifa, Israel

A new technique is presented for the calculation of the interaction of the inviscid external flow and the separated boundary layer in the case of the transonic flow over airfoils. A finite-difference method is used for the boundary-layer solution. On the forward portion of the airfoil the boundary-layer equations are solved for a given pressure distribution boundary condition, while on the rear portion of the airfoil and beyond, where separated flow occurs, the equations are solved for a given displacement thickness distribution boundary condition. The inviscid transonic flow solution and the boundary-layer solution are matched by a local point relaxation algorithm. incorporating the two methods of boundary-layer equations solution. Results are obtained for separated laminar, transitional, and turbulent flows on circular-arc airfoils at zero angle of attack. These results are in good agreement with available experimental data. The effects of Reynolds and Mach numbers are also examined.

Nomenclature

C_f = skin friction coefficient $= \tau_w / 0.5\rho_\infty U_\infty^2$
C_p = pressure coefficient $= (p - p_\infty)/0.5\rho_\infty U_\infty^2$
c_p = specific heat constant at constant pressure
D = doublet strength
$F(x)$ = airfoil shape function
H = total enthalpy $= c_p T + U^2/2$
K = transonic similarity parameter, $= (1 - M_\infty^2)/\delta_r^{2/3}$
L = chord length
M = Mach number
P = pressure
$\boldsymbol{P}$ = $(p_1,\ldots,p_n)$ vector of pressure at mesh points
$\boldsymbol{P}(\boldsymbol{\delta})$ = $(p_1,\ldots,p_n)$ $(\delta_1,\ldots,\delta_n)$; $\boldsymbol{P}$ depends on $\boldsymbol{\delta}$ and we denote this by $\boldsymbol{P}(\boldsymbol{\delta})$ or $(p_1,\ldots,p_n)$ $(\delta_1,\ldots,\delta_n)$
Pr = Prandtl number, taken as $Pr = 0.72$
Pr_t = turbulent Prandtl number, taken as $Pr_t = 0.9$
R = universal gas constant
Re = Reynolds number based on chord length
T = absolute temperature
U = velocity
$\hat{u}, \hat{v}$ = Cartesian perturbation velocities of the inviscid flow
u, v = components of velocity of the boundary layer in x and y directions, respectively
x, y = coordinates along and normal to airfoil and wake's centerline, respectively
X, Y = Cartesian coordinates
$\hat{Y}$ = transonic lateral coordinates, $= \delta_r^{1/3} Y$
γ = ratio of specific heats
δ_r = thickness ratio of airfoil
δ = displacement thickness $\int_0^\infty \left(1 - \frac{\rho u}{\rho_e u_e}\right) dy$
$\boldsymbol{\delta}$ = $(\delta_1,\ldots,\delta_n)$ vector of displacement thickness at mesh points
ϵ_m = kinematic eddy viscosity
ϵ_h = kinematic eddy conductivity
μ = viscosity
ν = kinematic viscosity
$\xi\eta$ = dummy integration variable
ρ = density
τ = shear stress
ϕ = perturbation potential
ψ = streamfunction
ω = relaxation parameter

Superscripts

(i) = iteration number
$\bar{(\ )}$ = time average value
$(\ )'$ = differentiation
$\tilde{(\ )}$ = nondimensional value
$(\ )^*$ = particular value

Subscripts

B = boundary-layer value
c = centerline of the wake
e = outer edge of the boundary layer
ex = external inviscid flow value
i = mesh points index in x direction
ℓ = index of transition point from the direct boundary-layer method to the inverse method
n = number of boundary layer mesh points in x direction
w = wall value
∞ = freestream value
0 = reference value

Introduction

RAPID progress has been made in recent years in the development of computational methods for inviscid transonic flows over two-dimensional airfoils. The results obtained by these methods differ from experimental data near the shock-wave location, especially for low Reynolds numbers as well as for airfoils at high lift coefficients. The predicted shock-wave location is too far downstream and its strength is too high. These differences are caused by viscous effects near the surface of the airfoil. If the shock wave is strong enough, separated flow occurs in the rear portion of the airfoil and in its wake, and the viscous layer thickens rapidly.

The external transonic inviscid flowfield, which is governed by mixed elliptic and hyperbolic partial differential equations, depends strongly on the boundary condition over the rear portion of the airfoil and its wake. This boundary condition simultaneously must satisfy the inviscid flow and the boundary-layer boundary-value problems.

Received Dec. 22, 1978; revision received Oct. 17, 1980.

*Graduate Student, Amelia Earhart Fellow, 1977/78; Department of Aeronautical Engineering.

†Professor, Lady Davis Chair in Experimental Aerodynamics; Department of Aeronautical Engineering. Associate Fellow AIAA.

The conventional inviscid/boundary-layer matching procedure to determine this boundary condition is divergent when separation occurs, since the boundary-layer solution with prescribed pressure distribution boundary condition is singular at the separation point, giving there a displacement thickness with an infinite slope. However, the solution of the boundary layer is regular at separation, when the displacement thickness is prescribed as a boundary condition. This was first demonstrated by Catherall and Mangler[1] and later by Carter,[2] Carter and Wornom,[3] Williams,[4] and Cebeci.[5] Similarly, regular solutions at separation can be obtained by prescribing the transverse component of velocity at the boundary-layer edge, as was shown by Klineberg and Steger[6] and by Tai[7]; or by prescribing the skin friction, as was demonstrated by Kuhn and Nielsen,[8] Klineberg and Steger,[9] Horton,[10] and Carter.[2]

The use of inverse boundary-layer methods in conjunction with integral techniques for computation of separated viscous-inviscid interaction at transonic speeds is presented by Klineberg and Steger,[6] Kuhn and Nielsen,[8] Tai,[7] and Theide.[11] The present investigation presents a new method for the computation of separated viscous-inviscid interactions at transonic speeds. This method is based on the coupling of the direct and inverse finite-difference boundary-layer procedures with the finite-difference solution of the small disturbance equations of the transonic inviscid flow.

Inviscid Flow

The external transonic flowfield is considered to be irrotational and is approximated by the small disturbance theory for slender airfoils.

By introducing a velocity potential function ϕ defined by $\hat{u}=\phi_X$; $\hat{v}=\phi_Y$, the basic transonic equation can be written as

$$[K-(\gamma+1)\phi_X]\phi_{XX}+\phi_{\hat{Y}\hat{Y}}=0 \tag{1}$$

where $K=(1-M_\infty^2)/\delta_r^{2/3}$, δ_r is the airfoil thickness ratio and $\hat{Y}$ is a scaled coordinate $\hat{Y}=\delta_r^{1/3}Y$.

A "displacement body" concept is employed for the determination of the inviscid edge, according to which the influence of the boundary layer on the inviscid stream is modeled as inviscid flow on the surface formed by adding the displacement thickness to the original surface geometry.

The boundary conditions of tangent flow are applied in the plane of the wing $\hat{Y}=0$. The conditions are

$$\begin{aligned}\phi_{\hat{Y}}(X,0) &= 0 && X<-1\\ &= \left(F(X)+\frac{\delta(X)}{\delta_r}\right) && -1<X<1\\ &= \frac{\delta'(X)}{\delta_r} && X>1\end{aligned} \tag{2}$$

where the body shape is given by $Y=\delta_r F(X)$, $|X|<1$, and $\delta(X)$ is the displacement thickness.

The far-field analytical solution is used as a boundary condition and is given by

$$\phi(X,\hat{Y})=\left(\frac{1}{2\pi K^{1/2}}\right)\frac{DX}{X^2+K\hat{Y}^2}+\ldots \tag{3}$$

where the doublet strength D is

$$D=2\int_{-1}^{+1}F(\xi)\,d\xi+2\int_{-1}^{\infty}\left(\frac{\delta(\xi)}{\delta_r}\right)d\xi+\frac{\gamma+1}{2}\int\int_{-\infty}^{+\infty}\hat{u}^2\,d\xi\,d\eta \tag{4}$$

This set of equations with the corresponding boundary conditions is solved by a computer program originally developed by Murman and Cole[12] and later modified to its conservative form by Murman.[13] The program uses mixed finite-difference equations that are solved by a line relaxation algorithm.

Viscous Flow

The first-order boundary-layer equations are used for describing the viscous flow region. The governing equations for a compressible laminar or turbulent boundary layer in coordinates parallel and normal to the surface are

Continuity:

$$\frac{\partial}{\partial x}(\bar{\rho}\bar{u})+\frac{\partial}{\partial y}(\bar{\rho}\bar{v})=0 \tag{5a}$$

Momentum:

$$\bar{\rho}\bar{u}\frac{\partial\bar{u}}{\partial x}+\bar{\rho}\bar{v}\frac{\partial\bar{u}}{\partial y}=-\frac{d\bar{P}}{dx}+\frac{\partial}{\partial y}\left[\mu\frac{\partial\bar{u}}{\partial y}-\bar{\rho}\bar{u}\bar{v}\right] \tag{5b}$$

Energy:

$$\bar{\rho}\bar{u}\frac{\partial\bar{H}}{\partial x}+\bar{\rho}\bar{v}\frac{\partial\bar{H}}{\partial y}=\frac{\partial}{\partial y}\left[\mu\left(1-\frac{1}{Pr}\right)\bar{u}\frac{\partial\bar{u}}{\partial y}+\frac{\bar{\mu}}{Pr}\frac{\partial\bar{H}}{\partial y}-\bar{\rho}\bar{v}\bar{H}\right] \tag{5c}$$

where

$$\bar{H}=c_p\bar{T}+\tfrac{1}{2}\bar{u}^2$$

The boundary conditions at the wall are

$$\bar{u}(x,0)=0;\quad \bar{v}(x,0)=0 \tag{6a}$$

$$\frac{\partial\bar{H}}{\partial y}(x,0)=0 \text{ adiabatic wall condition} \tag{6b}$$

The boundary conditions at the wake's centerline ($y=0$; $x>1$) are

$$\frac{\partial\bar{u}}{\partial y}(x,0)=0;\ \bar{v}(x,0)=0 \text{ symmetric flow conditions} \tag{7a}$$

$$\frac{\partial\bar{H}}{\partial y}(x,0)=0 \text{ symmetric flow conditions} \tag{7b}$$

the external freestream flow conditions are

$$\frac{\partial\bar{u}}{\partial y}=0 \tag{8a}$$

$$\frac{\partial\bar{H}}{\partial y}=0 \tag{8b}$$

In addition it is assumed that the ideal gas state equation: $P/\rho=\gamma RT$, is applicable as well as the Sutherland's law relating viscosity to temperature.

For a turbulent flow an eddy viscosity and an eddy conductivity concept is assumed

$$-\bar{\rho}\bar{u}\bar{v}=\bar{\rho}\epsilon_m\frac{\partial\bar{u}}{\partial y} \tag{9a}$$

$$-\bar{\rho}\bar{v}\bar{H}=\bar{\rho}\epsilon_h\frac{\partial\bar{H}}{\partial y}\equiv\bar{\rho}\frac{\epsilon_m}{Pr_t}\frac{\partial\bar{H}}{\partial y} \tag{9b}$$

where Pr_t is a turbulent Prandtl number taken as $Pr_t=0.90$.

The Cebeci-Smith mixing length model[14] has been used in this study on the airfoil. In the wake the following eddy viscosity model has been used:

$$\epsilon_m = 0.001176\delta\,|u_\delta - u_c|$$

where δ is the displacement thickness and u_δ and u_c are the velocities at the edge and at the centerline of the wake, respectively.

The set of partial-differential equations, the boundary conditions, and a specified pressure distribution $P(x)$ define the "direct (boundary layer) problem." If, instead of a specified pressure distribution, the displacement thickness distribution $\delta(x)$ is specified, "the inverse (boundary layer) problem" is defined. In the present study the boundary-layer program was written to solve the direct problem up to a certain x point, an input parameter, and then switched to solve the inverse problem.

The direct problem was solved by a slight modification of the Cebeci-Keller method.[14] This method, as presented in Ref. 14, resulted in a numerically unstable solution (for each x point, the solution was oscillatory in the vicinity of the external freestream edge). The instability was removed by reordering the coefficient matrix corresponding to the energy equation (Ref. 19, Appendix A). The reordering apparently caused the block dominance condition to be satisfied.[16]

The inverse boundary layer problem was solved by an extension of the Cebeci method[5] for the solution of the incompressible inverse boundary-layer problem, to the solution of the compressible boundary-layer problem. We introduce the standard nondimensional coordinates $\tilde{y}=y(Re)^{1/2}/L$; $\tilde{x}=x/L$ and the standard nondimensional variables denoted by $(\tilde{\ })$, with reference values u_0, ρ_0, μ_0. Using the streamfunction ψ defined by $\tilde{\rho}\tilde{u}=\partial\psi/\partial y$; $\tilde{\rho}\tilde{v}=-\partial\psi/\partial x$, we get the equations:

Momentum:

$$\psi'\frac{\partial}{\partial\tilde{x}}\left(\frac{1}{\tilde{\rho}}\psi'\right)-\frac{\partial\psi}{\partial\tilde{x}}\left(\frac{1}{\tilde{\rho}}\psi'\right)'=-\frac{d\tilde{P}}{d\tilde{x}}+\left[b\left(\frac{1}{\tilde{\rho}}\psi'\right)'\right]'$$

Energy:

$$\psi'\frac{\partial\tilde{H}}{\partial\tilde{x}}-\frac{\partial\psi}{\partial\tilde{x}}\tilde{H}'=\left\{\left(1-\frac{1}{Pr}\right)\tilde{\mu}\frac{1}{\tilde{\rho}}\psi'\left(\frac{1}{\tilde{\rho}}\psi'\right)'+\frac{\tilde{\mu}}{Pr}\left(1+\frac{\epsilon_m^+ P_r}{Pr_t}\right)\tilde{H}'\right\}' \tag{10}$$

where

$$b=\tilde{\mu}(1+\epsilon_m^+);\quad \epsilon_m^+=\frac{\epsilon_m}{\tilde{\nu}}=\frac{\bar{\epsilon}_m}{\tilde{\nu}};\quad \tilde{H}=\tilde{T}+\frac{1}{2}\tilde{u}^2$$

and $(\,)'$ is the derivative with respect to $\tilde{y}$.

The wall boundary conditions are

$$\psi(\tilde{x},0)=0;\quad \psi'(\tilde{x},0)=0 \text{ at the wall}$$

$$\left(\frac{\psi'(\tilde{x},0)}{\tilde{\rho}(\tilde{x},0)}\right)'=0 \text{ at the wake centerline; } \tilde{H}'(\tilde{x},0)=0 \tag{11a}$$

The external boundary conditions are

$$\psi(\tilde{x},\tilde{y}_e)=\tilde{\rho}_e\tilde{u}_e[\tilde{y}_e-(Re)^{1/2}/L\delta(\tilde{x})]$$

$$\psi'(\tilde{x},\tilde{y}_e)=\tilde{\rho}_e\tilde{u}_e;\quad \tilde{H}'(\tilde{x},\tilde{y}_e)=0 \tag{11b}$$

Equations (10) and boundary conditions Eqs. (11) are transformed to a set of first-order differential equations and then solved by the finite-difference box method of Cebeci and Keller,[14] with a nonuniform geometric net spacing. The initial values at the first station are supplied by the direct problem solution and the initial values at the other stations are taken as a linear extrapolation of the values of two preceding x stations. (This is a modification of the method in Ref. 14.) The inverse boundary-layer method is described in detail in Ref. 15.

In order to remove the well-known instability encountered in solving the boundary-layer equations in the direction opposite to the local flow direction, the approximation first introduced by Reyhner and Flügge-Lotz[17] is used. The streamwise convection terms $\rho u(\partial u/\partial x)$ and $\rho u(\partial H/\partial x)$ are neglected in the reverse flow region.

Numerical difficulties appeared in imposing discontinuous surface boundary conditions at the trailing edge: the solution of the boundary-layer equations did not converge with the wake centerline boundary conditions imposed directly at the first wake x station. In order to remove this difficulty the passage from the airfoil to the wake is done by a two-step method: 1) the boundary-layer equations are first solved at the initial wake station with wall boundary conditions

$$u(x,0)=0;\quad v(x,0)=0;\quad \frac{\partial H}{\partial y}(x,0)=0$$

and 2) the solution obtained in step 1 is used as an initial value for the solution of the boundary layer equations with the correct boundary conditions

$$\frac{\partial u}{\partial y}(x,0)=0;\quad v(x,0)=0;\quad \frac{\partial H}{\partial y}(x,0)=0$$

The first-order boundary-layer equations are proper for describing the viscous flow region for laminar flows.[18,19] For turbulent flows, however, studies of Melnik and Chow[20] show that normal pressure gradients across the boundary layer are important near the trailing edge and must be retained in a consistent description of the flow there. Melnik and Chow[21] have found that for turbulent flows over lifting airfoils, the first-order boundary-layer equations approximation accounts for only about 50% of the viscous effect on lift. The remaining contribution arising from normal pressure gradients near the trailing edge, due to surface and wake curvature. Unfortunately, the Melnik-Chow theory applies only to cusped trailing edges and no corresponding theory is available for the wedged shaped trailing edges considered in the present work. However, the present investigation is aimed primarily at demonstrating the applicability of the new interaction matching method for separated flows, and therefore, the effect of the normal pressure gradients has been neglected. The effect of the normal pressure gradient should be included in further development of this calculation method.

Viscous-Inviscid Interaction

In calculating the viscous-inviscid interaction, it is assumed that the effect of the boundary layer on the external inviscid flow can be approximated by adding the displacement thickness to the airfoil surface geometry, and computing the inviscid flow over that body. The external inviscid flow solution provides a pressure distribution $P_{ex}(x)$ that is related to the displacement thickness distribution $\delta(x)$ by a functional relation

$$P_{ex}(x)=P_{ex}(\delta(x)) \tag{12}$$

The classical approach of calculating viscous inviscid interactions is to compute the boundary layer for a prescribed pressure distribution. This approach cannot be used for flows with separated flow regions because the solution of the

boundary-layer equations for a given pressure distribution is singular at the separation point and the computation cannot proceed beyond this point. However, it is possible to compute boundary layers with separated flow regions when the displacement thickness is prescribed in advance. The pressure distribution in this case is determined directly as a part of the boundary-layer solution.

The following functional relation between the boundary-layer pressure distribution $P_B(x)$ and the displacement thickness distribution $\delta(x)$ holds:

$$P_B(x) = P_B[\delta(x)] \tag{13}$$

The matching problem is to find a particular $\delta^*(x)$ that satisfies the equation

$$P_B(\delta^*(x)) = P_{ex}(\delta^*(x)) \tag{14}$$

Therefore, a particular vector $\delta^* = (\delta_1^*, \delta_2^*, \ldots, \delta_n^*)$ must be found such that the vectors

$$P_B = (P_{B,1}, P_{B,2}, \ldots, P_{B,n})(\delta_1^*, \delta_2^*, \ldots, \delta_n^*)$$

and

$$P_{ex} = (P_{ex,1}, P_{ex,2}, \ldots, P_{ex,n})(\delta_1^*, \delta_2^*, \ldots, \delta_n^*)$$

satisfy the relation

$$P_{ex,i} = P_{B,i} \quad \text{for } i = 1,2,\ldots,n \tag{15}$$

Although the problem is rather complicated, a two-dimensional simplified picture can be used to visualize the problem, as suggested by Brune et al.,[22] and illustrated in Figs. 1 and 2.

The new matching technique couples the direct and inverse finite-difference boundary-layer procedures with the finite-difference inviscid transonic flow solution and iterates them to convergence. The matching procedure is based on the assumption that the relation between $P_{ex}(x)$ and $\delta(x)$ and between $P_B(x)$ and $\delta(x)$ is two dimensional, i.e., for each i, $P_{ex,i}$ depends only on δ_i (and not on δ_j, $j \neq i$) and $P_{B,i}$ depends only on δ_i.

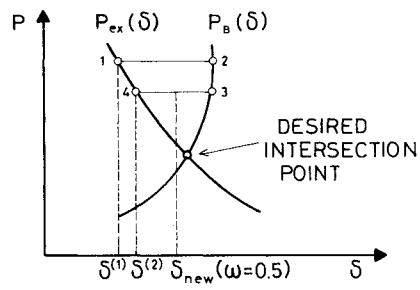

Fig. 1 The relaxation method in the forward portion of the airfoil.

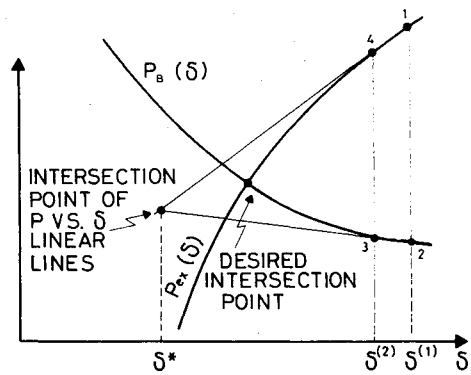

Fig. 2 The relaxation method in the rear portion of the airfoil and beyond.

This iterative procedure consists of the following steps:

1) Select an initial value $\delta^{(1)}(x)$ and compute the inviscid pressure distribution $P_{ex}^{(1)}(x)$ for a given displacement thickness distribution $\delta_{ex}^{(1)}(x)$ where $\delta_{ex}^{(1)}(x) \equiv \delta^{(1)}(x)$. The result of this step is the set of points $(\delta_{ex,i}^{(1)}; P_{ex,i}^{(1)})_{i=1,2,\ldots,n}$ represented by point 1 in Figs. 1 and 2.

2) On the forward portion of the airfoil, up to a certain x station, solve the direct boundary-layer problem for the preceding pressure distribution $-P_{ex}^{(1)}$ boundary condition, and compute the corresponding displacement thickness distribution $\delta_B^{(1)}(x)$. From that point on, solve the inverse boundary-layer problem for a given displacement thickness distribution $\delta_B^{(1)}(x)$, where $\delta_B^{(1)}(x) \equiv \delta_{ex}^{(1)}(x)$ and obtain the corresponding pressure distribution $P_B^{(1)}(x)$. The result of this step are the following sets of points:

$$(\delta_{B,i}^{(1)}; P_{ex,i}^{(1)})_{i=1,2,\ldots,\ell-1} \text{ (point 2 on Fig. 1)}$$
$$(\delta_{ex,i}^{(1)}; P_{B,i}^{(1)})_{i=\ell,\ell+1,\ldots,n} \text{ (point 2 on Fig. 2)}$$

3) and 4) Repeat steps 1 and 2 for some other displacement thickness distribution $\delta^{(2)}(x)$. The result of these steps are the following sets of points:

$$(\delta_{ex,i}^{(2)}; P_{ex,i}^{(2)})_{i=1,2,\ldots,n} \text{ (point 4 on Figs. 1 and 2)}$$
$$(\delta_{B,i}^{(2)}; P_{ex,i}^{(2)})_{i=1,2,\ldots,\ell-1} \text{ (point 3 on Fig. 1)}$$
$$(\delta_{ex,i}^{(2)}; P_{B,i}^{(2)})_{i=\ell,\ell+1,\ldots,n} \text{ (point 3 on Fig. 2)}$$

5) A new displacement thickness distribution δ_{new} is obtained in the following way: In the forward portion of the airfoil δ_{new} is taken as

$$\delta_{new,i} = \omega\delta_{B,i}^{(2)} + (1-\omega)\delta_{ex,i}^{(2)} \quad \text{for } i = 1,2,\ldots,\ell-1$$

where ω is a relaxation parameter (see Fig. 1). In the rear portion of the airfoil and in the wake δ_{new} is taken as

$$\delta_{new,i} = \omega\delta_i^* + (1-\omega)\delta_i^{(2)} \quad \text{for } i = \ell,\ell+1,\ldots,n$$

where $\{\delta_i^*\}_{i=\ell,\ell+1,\ldots,n}$ are the intersection points of the pressure vs δ linear lines, as is shown in Fig. 2; i.e., the intersection of the linear line that passes through

$$(\delta_{ex,i}^{(1)}; P_{ex,i}^{(1)}); \quad (\delta_{ex,i}^{(2)}; P_{ex,i}^{(2)})$$

with the linear line that passes through

$$(\delta_{ex,i}^{(1)}; P_{B,i}^{(1)}); \quad (\delta_{ex,i}^{(2)}; P_{B,i}^{(2)}), \quad \text{for } i = \ell,\ell+1,\ldots,n$$

The process is recycled by replacing $\delta^{(2)}$ by δ_{new} and going back to step 3 while $\delta^{(1)}$ is held fixed. This process continues until convergence is obtained; at every point on the forward portion of the airfoil, $\delta_B^{(2)}$ differs from $\delta_{ex}^{(2)}$ by less than a specified tolerance, and at every point on the rear portion of the airfoil and the wake $P_B^{(2)}$ differs from $P_{ex}^{(2)}$ by less than some other specified tolerance.

The relaxation parameter ω is chosen small enough to prevent oscillations. It was found that its value depends on the interaction strength; the stronger the interaction, the smaller is the required value of the relaxation parameter. The present method requires two initial-guess functions $\delta^{(1)}$ and $\delta^{(2)}$. These are selected following the suggestion of Werle and Davis,[23] as the corresponding displacement thickness distribution of two lower heights of the profile, well below the value at which separation occurs.

At first an alternate procedure was examined; steps 1-5 were the same but the recycling procedure continued by replacing $\delta^{(1)}$ by $\delta^{(2)}$ and $\delta^{(2)}$ by δ_{new}. This procedure experienced severe convergence problems. The displacement

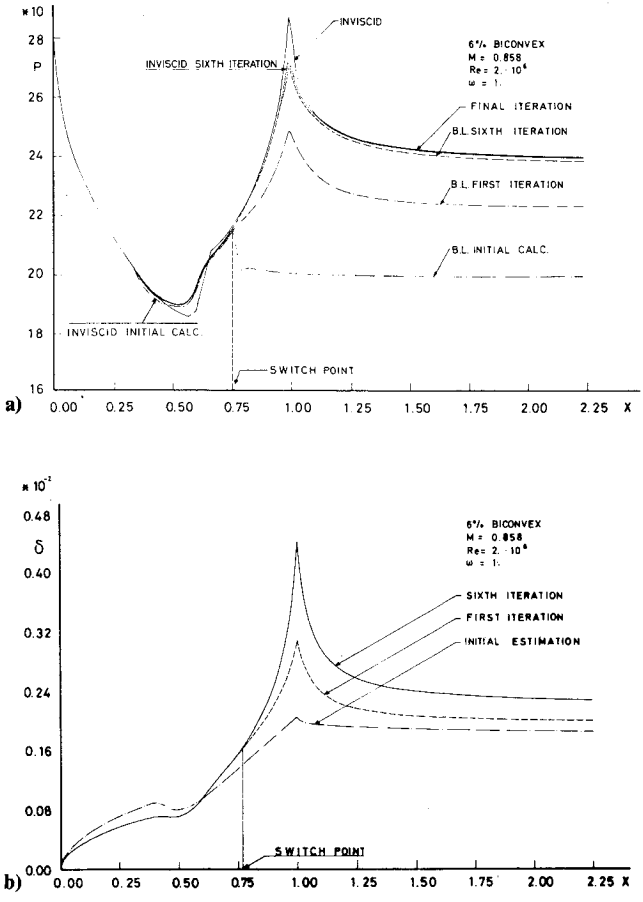

Fig. 3 a) Pressure distributions of the convergence procedure; and b) displacement thickness distributions of the convergence procedure.

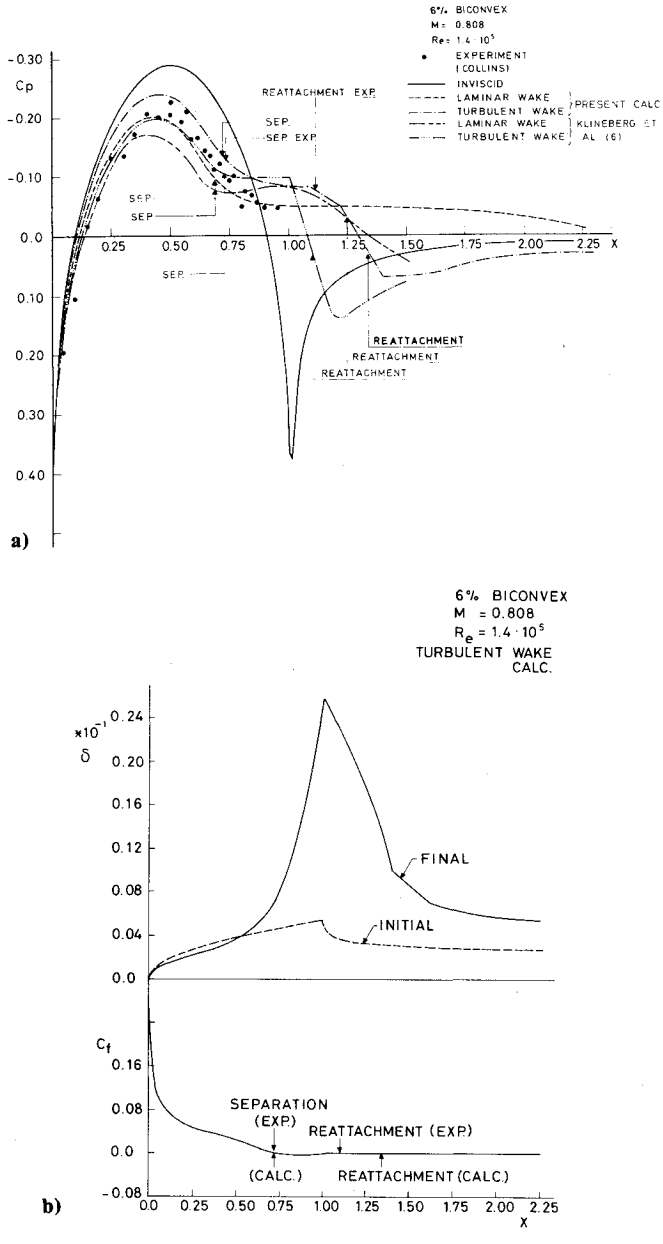

Fig. 4 a) Pressure coefficient distributions; and b) displacement thickness and skin friction coefficient distributions.

thickness distribution tended after several iterations to oscillate or even to diverge, and the pressure distribution of the external inviscid flow tended after several iterations to oscillate with the oscillations range increasing with the iteration number. These difficulties were corrected by the present procedure; namely, one of the displacement thickness distributions is held fixed, while the second, latest found displacement thickness distribution is replaced after each cycle by the new approximation. This modification prevents oscillations related to using two successive displacement thickness distributions with incorrect, opposite in direction local curvatures, to get a new approximation. It also prevents possible oscillations or divergence due to the fact that the matching problem is not a two-dimensional one, as assumed by using a two-dimensional $P-\delta$ relation. Improving the convergence at one station can worsen the convergence at some other station, thus causing oscillations or even divergence.

The switch point from the direct method to the inverse method is placed between the point of minimum pressure and the separation point. The discontinuity in the displacement thickness distribution that occurs at the interface between the direct and the inverse regions does not cause any difficulty. This discontinuity is corrected through the updating procedure and it disappears as the procedure continues.

When there is a shock wave, the shock wave is spread over several mesh points.[12] For turbulent flows the iteration procedure was applied through the shock wave without any difficulty. However, for laminar flows some difficulty appeared in the initial cycles; the two displacement thickness distributions did not give a good resolution of the dependence of the pressure on the displacement thickness near the base of the shock wave. In order to overcome this difficulty, the forward updated displacement thickness distribution was joined in the initial cycles, to the rear updated displacement thickness distribution by a smooth continuation across the shock wave. Figures 3a and 3b show the convergence procedure as obtained for a 6% biconvex airfoil at $M=0.858$, $Re=2\times10^6$ and a turbulent flow.

Results and Discussion

Interaction computations with the present matching technique were made for the test conditions of the experimental data of Collins (presented by Klineberg and Steger[6]) and of Knechtel.[24] Calculations were also made for a range of Mach numbers and for a range of Reynolds numbers, to study their effect in turbulent flows over biconvex airfoils. Experimental data is not available at present for these computations.

Calculations were performed for the test conditions of the experiments of Collins[6] with 1) flow over a 6% biconvex airfoil at Mach number $M=0.808$ and Reynolds number $Re=1.4\times10^5$ and 2) flow over a 12% biconvex airfoil at Mach number $M=0.78$ and Reynolds number $Re=3.6\times10^4$.

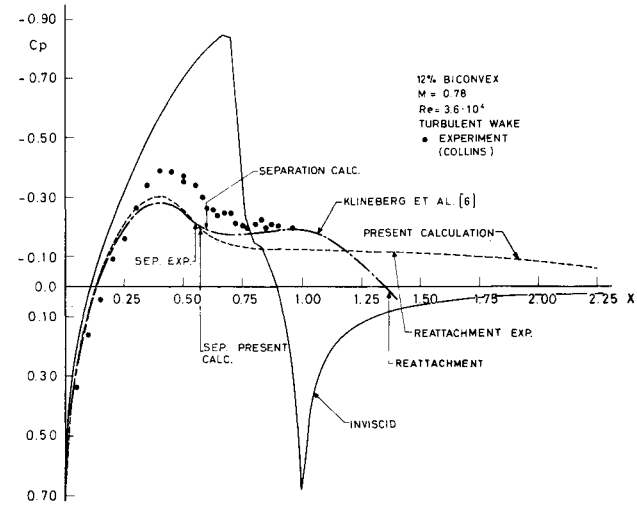

Fig. 5 Pressure coefficient.

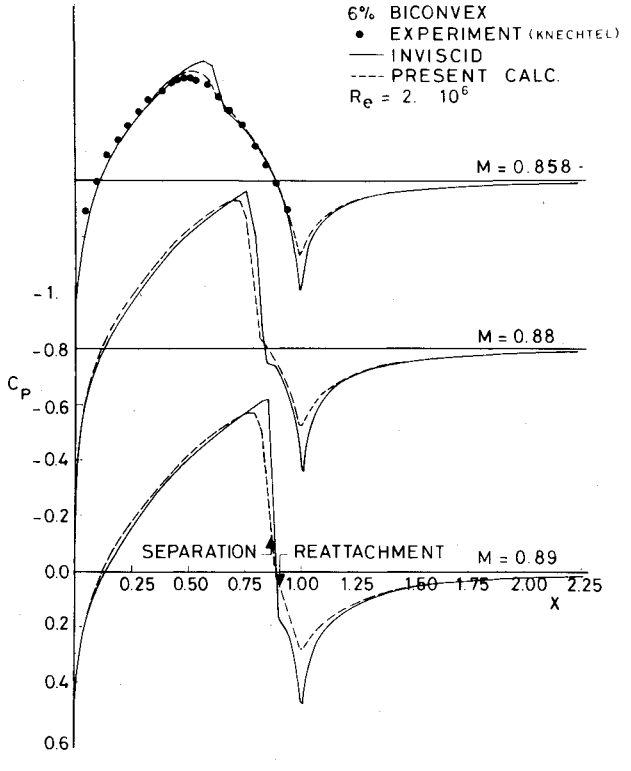

Fig. 6 Effect of Mach number on pressure coefficient.

At these flow conditions of low transonic Mach numbers and relatively high Reynolds numbers, the wake can be assumed to be turbulent.[6] Therefore, calculations for these flow conditions were performed with a turbulent modeled wake. In order to study the effect of the wake model, the first example was calculated also with a laminar modeled wake.

Some difficulty appeared in trial runs of these very strong interaction calculations; the converged displacement thickness distribution was oscillatory at the wake region, with maximum and minimum values following the mesh points. This phenomena did not appear in the fully turbulent examples that will be described later, in which the interaction strength is comparatively weak. It was found that the location of the peaks and the range of the oscillations depend on the method used for computing the slope of the effective body near the trailing edge. These oscillations were suppressed by using an upstream derivative to compute the slope of the effective body.

Figures 4a and 4b present the results of the pressure coefficients, the displacement thickness and the skin friction coefficient distributions of the 6% biconvex airfoil calculations. Figure 4a includes also the results of Klineberg and Steger[6] who used an integral boundary-layer method for their calculations. It can be seen that our calculated pressure coefficient is in reasonable agreement with the experimental results. The experimental results are found to be somewhat closer to our laminar modeled wake calculation than the turbulent modeled wake calculation. The separation point of the turbulent wake approximation coincides with the experimental data, while the reattachment point of the turbulent modeled wake computation is somewhat behind the measured reattachment position. Our results are in better agreement with the experimental data than those obtained by Klineberg and Steger.[6] This figure indicates also the upstream influence that exists in subsonic flows.

Figure 5 presents the results of the 12% biconvex airfoil example. These results indicate that the pressure coefficient obtained by the present calculations is somewhat low in comparison with the experimental data, but it is in good qualitative agreement. The position of the separation is predicted reasonably well but, contrary to the experimental results, the whole wake is predicted to remain separated. The numerical procedure converged to this solution and no attempt was made here to study the effect of a finer mesh. There are several possible reasons for these results: 1) The simple turbulence model used in the wake could be inadequate. 2) The transition point could be incorrect. Moving the transition point somewhat upstream would probably improve the results as obtained in the previous example. 3) The transonic small perturbation equations are an inaccurate approximation for a 12% thick airfoil. 4) The boundary-layer equations should be modified when there is a large region with reverse flow.

These computations required the use of an under-relaxation parameter, ranging between 0.1-0.25, in the iterative computations. The calculations were made with 78×30 mesh points in the inviscid flowfield and 64 mesh points in the streamwise direction, in the boundary layer computation. As an indication of the computer time, convergence was obtained in the 6% biconvex airfoil example with the turbulent wake approximation, using an under-relaxation parameter $\omega=0.25$ after 44 iterations, requiring about 11 min CPU time on a AMDAHL computer.

The experimental test conditions of Knechtel[24] are flow over a 6% biconvex airfoil at Mach number $M=0.858$ and Reynolds number $Re=2\times10^6$. At these flow conditions of high Reynolds number and low, transonic Mach number the flow appears to be turbulent. Therefore, calculations for this example, as well as for the following computation, were made with a turbulent boundary layer. The transition point in these calculations were taken as $x=0.4$. The result of this calculation is presented by one of the graphs of Fig. 6. As observed from this graph, the calculated pressure coefficient is in good agreement with the experimental data, although it is somewhat high near the shock wave location. This may be attributed to the fact that the normal pressure gradients are neglected in these calculations.

The effect of Mach number is presented in Fig. 6. These computations were made for flow over a 6% biconvex airfoil at Reynolds number $Re=2\times10^6$ with a turbulent boundary layer at Mach number $M=0.858$, 0.88, and 0.89. As observed from these results, the effect of the boundary layer on the inviscid flow solution is to reduce the pressure gradients near the trailing edge, to move the shock wave position somewhat upstream, to reduce its strength and to smooth its base. These effects become stronger as the Mach number is increased. These trends are in agreement with known experimental data.

Figures 7a and 7b present the effect of Reynolds number as obtained for a 6% biconvex airfoil at Mach number $M=0.87$ with a turbulent boundary layer, for Reynolds numbers $Re=1\times10^6$; 2×10^6; 4×10^6 and 8×10^6. As the Reynolds

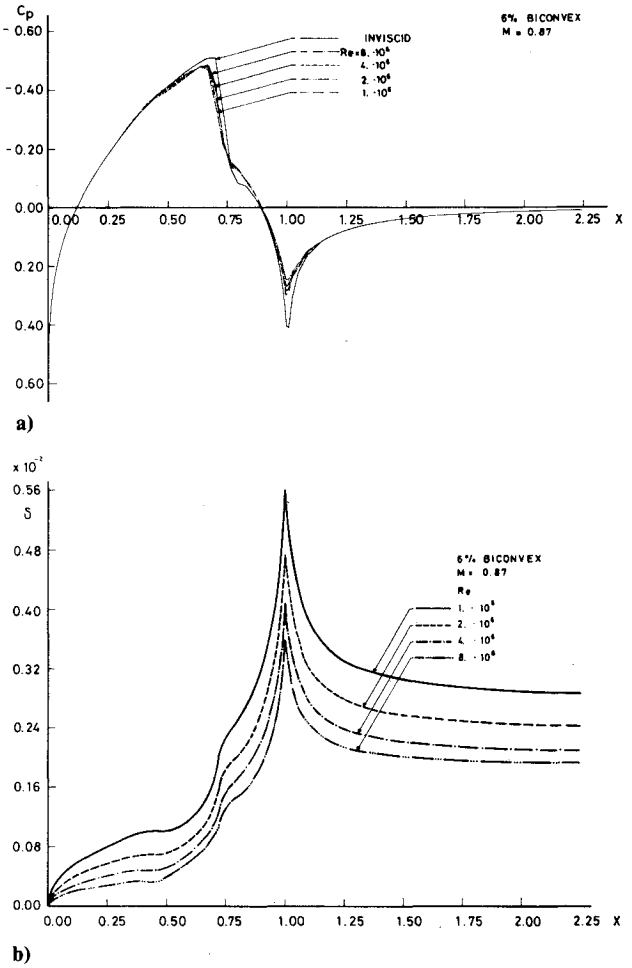

Fig. 7 a) Effect of Reynolds number on pressure coefficients; and b) effect of Reynolds number on displacement thickness distribution.

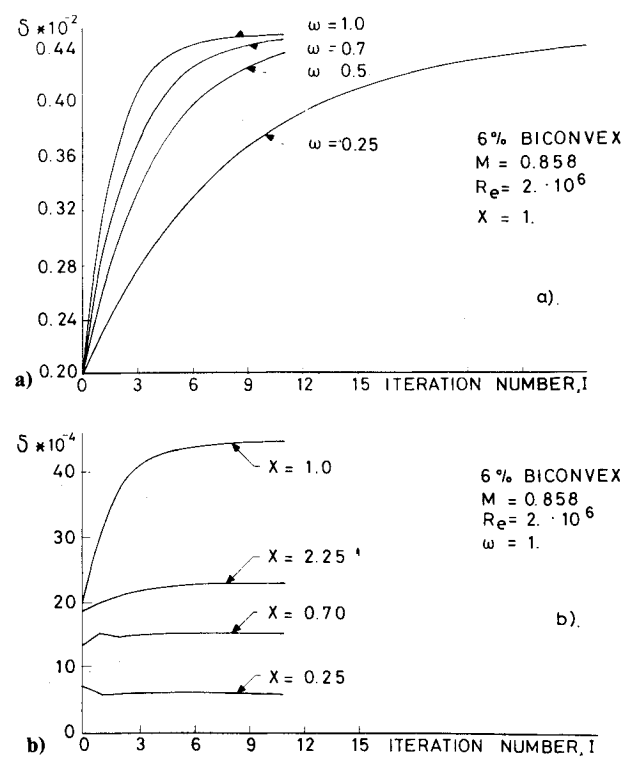

Fig. 8 Convergence of the displacement thickness calculation: a) at different locations; and b) at $x=1$, for different relaxation parameters.

number decreases, the displacement thickness distribution becomes thicker, and the interaction strength on the inviscid pressure coefficient increases, although the effect of change in Reynolds number for turbulent boundary layers is quite small. These results are in accordance with experimental data of Ackeret et al.[25] and of Holder.[26]

These turbulent flow calculations, where the interaction strength is weak, were run with a relaxation parameter $\omega=1$. The calculations converged in about 8-11 iterations, requiring about 5-7 min CPU computer time on a AMDAHL 470 computer.

Figure 8a presents the convergence of the displacement thickness at different locations as obtained from the calculation for the 6% biconvex airfoil at Mach number $M=0.858$, Reynolds number $Re=2\times10^6$, and a turbulent boundary layer, with a relaxation parameter $\omega=1$. Figure 8b presents the convergence of the displacement thickness at $x=1$ for different relaxation parameters. These results were obtained for a 6% biconvex airfoil, Mach number $M=0.858$, Reynolds number $Re=2\times10^6$ with a turbulent boundary layer. As observed from this figure, the convergence rate increases quickly as the relaxation parameter is increased, but it must be chosen small enough to prevent oscillations.

Concluding Remarks

A simple, powerful method for matching the external inviscid flow with a separated boundary layer has been presented. This method has been applied to the calculation of the interaction at transonic flow over a symmetric, biconvex airfoil, at zero angle of attack, with a laminar, transitional, or turbulent boundary layer. Comparison of some of the results with available experimental data shows quite good agreement.

The method can be extended to include normal pressure gradients across the boundary layer in the case of turbulent flows and probably can also be applied to the lifting airfoil problem. Further research is required to investigate the effect of the mesh spacing refinement near the trailing edge and the effect of an approximate correction to the boundary-layer equations at the trailing edge of airfoils having a small trailing-edge angle.

Acknowledgments

This research is part of the first author's D.Sc. Thesis in Aeronautical Engineering presented to the Senate of the Technion-Israel Institute of Technology. The authors are indebted to J. D. Cole for his advice and to R. T. Davis and M. Werle for helpful discussions. The authors are also grateful to the Computer Sciences Department at Purdue University and the Department of Mathematical Sciences at the University of Cincinnati for providing the authors with the use of their computer facilities.

References

[1] Catherall, D. and Mangler, K. W., "The Integration of the Two-Dimensional Laminar Boundary-Layer Equations Past the Point of Vanishing Skin Friction," *Journal of Fluid Mechanics*, Vol. 26, Sept. 1966, pp. 163-182.

[2] Carter, J. E., "Solution for Laminar Boundary Layers with Separation and Reattachment," AIAA Paper 74-583, June 1974.

[3] Carter, J. E. and Wornom, S. F., "A Forward Marching Procedure for Separated Boundary-Layer Flows," *AIAA Journal*, Vol. 13, Aug. 1975, pp. 1101-1103.

[4] Williams, P. G., "A Reverse Flow Computation in the Theory of Self-Induced Separation," *Proceedings of the 4th International Conference on Numerical Methods in Fluid Dynamics*, Vol. 35, *Lectures Notes in Physics*, edited by R. D. Richtmyer, Springer Verlag, New York, 1975, pp. 445-451.

[5] Cebeci, T., "Separated Flows and their Representation by Boundary-Layer Equations," Rept. ONR-CR 215-234-2, Sept. 1976.

[6] Klineberg, J. M. and Steger, J. L., "Calculation of Separated Flows at Subsonic and Transonic Speeds," *Proceedings of the 3rd International Conference on Numerical Methods in Fluid Mechanics*, Vol. 2, Springer Verlag, Berlin, 1973, pp. 161-168.

[7] Tai, T. C., "Transonic Laminar Viscous-Inviscid Interaction over Airfoils," *AIAA Journal*, Vol. 13, Aug. 1975, pp. 1065-1072.

[8] Kuhn, G. D. and Nielsen, J. N., "Prediction of Turbulent Separated Boundary Layers," AIAA Paper 73-663, July 1973.

[9] Klineberg, J. M. and Steger, J. L., "On Laminar Boundary-Layer Separation," AIAA Paper 74-94, Jan.-Feb. 1974.

[10] Horton, H. P., "Separating Laminar Boundary Layers with Prescribed Wall Shear," *AIAA Journal*, Vol. 12, Dec. 1974, pp. 1772-1774.

[11] Thiede, P. G., "Prediction Method for Steady Aerodynamic Leading on Airfoils with Separated Transonic Flow," *Prediction of Aerodynamic Loading*, AGARD CP-204, Sept. 28-29, 1976.

[12] Murman, E. M. and Cole, J. D., "Calculation of Plane Steady Transonic Flows," *AIAA Journal*, Vol. 9, Jan. 1971, pp. 114-121.

[13] Murman, E. M., "Analysis of Embedded Shock Waves Calculated by Relaxation Methods," *AIAA Journal*, Vol. 12, May 1974, pp. 626-633.

[14] Cebeci, T. and Smith, A.M.O., *Analysis of Turbulent Boundary Layers*, Academic Press, 1974.

[15] Gordon, R., "Computation of Inviscid Transonic Flow-Boundary Layer Interaction Over a Symmetric Airfoil Without Lift," D.S.C. Thesis, presented to the Senate of the Technion, Isreal Inst. of Tech., 1979.

[16] Varah, J. M., "On the Solution of Block Tridiagonal Systems Arising from Certain Finite-Difference Equations," *Mathematics of Computation*, Vol. 26, No. 120, 1972, pp. 859-868.

[17] Reyhner, T. A. and Flügge-Lotz, I., "The Interaction of a Shock Wave with a Laminar Boundary Layer," *International Journal of Non-Linear Mechanics*, Vol. 3, No. 2, 1968, pp. 173-199.

[18] Brown, S. N. and Stewartson, K., "Trailing-Edge Stall," *Journal of Fluid Mechanics*, Vol. 42, July 1970, pp. 561-584.

[19] Brown, S. N. and Stewartson, K., "Wake Curvature and the Kutta Condition in Laminar Flow," *The Aeronautical Quarterly*, Vol. 26, Nov. 1975, pp. 275-280.

[20] Melnik, R. E. and Chow, R., "Asymptotic Theory of Two-Dimensional Trailing-Edge Flows," *NASA Conference on Aerodynamic Analysis Requiring Advanced Computers*, NASA CP 347, 1975, pp. 177-249.

[21] Melnik, R. E. and Chow, R., "Theory of Viscous Transonic Flow over Airfoils at High Reynolds Number," AIAA Paper 77-680, June 1977.

[22] Brune, G. W., Rubbert, P. E., and Nark, T. C. Jr., "A New Approach to Inviscid Flow/Boundary Layer Matching," AIAA Paper 74-601, June 1974.

[23] Davis, R. T. and Werle, M. J., private communication, 1977-78.

[24] Knechtel, E. D., "Experimental Investigation at Transonic Speeds of Pressure Distributions over Wedge and Circular Arc Airfoil Sections and Evaluation of Perforated-Wall Interference," NASA TND-15, 1959.

[25] Ackeret, J., Feldman, F., and Rott, N., "Investigation of Compression Shocks and Boundary Layers in Gases Moving at High Speeds," NACA TM 1113, Jan. 1947.

[26] Holder, D. W., "The Transonic Flow Past Two-Dimensional Airfoils," *Journal of the Royal Aeronautical Society*, Vol. 68, Aug. 1964, pp. 501-516.